

The equation of state of two dimensional Yang-Mills theory

Nikhil Karthik* and Rajamani Narayanan†

Department of Physics, Florida International University, Miami, FL 33199.

Abstract

We study the pressure, P , of $SU(N)$ gauge theory on a two-dimensional torus as a function of area, $A = l/t$. We find a cross-over scale that separates the system on a large circle from a system on a small circle at any finite temperature. The cross-over scale approaches zero with increasing N and the cross-over becomes a first order transition as $N \rightarrow \infty$ and $l \rightarrow 0$ with the limiting value of $\frac{2Pl}{(N-1)t}$ depending on the fixed value of Nl .

*Electronic address: nkarthik@fiu.edu

†Electronic address: rajamani.narayanan@fiu.edu

I. INTRODUCTION

The partition function for $SU(N)$ gauge theory on a 2d torus with spatial extent l and temperature t is only a function of the area, $A = l/t$, and is given by [1]

$$Z_N(A) = \sum_r \exp\left(-\frac{C_r^{(2)}l}{Nt}\right), \quad (1)$$

where $C_r^{(2)}$ is the value of Casimir in the representation r . One can arrive at (1) by taking the continuum limit of a lattice formalism on a finite lattice [2]. The asymptotic behavior at large N was studied in [3] where only representations with $C_r^{(2)}$ of $\mathcal{O}(N)$ dominate. Since the partition function is a sum over string like states with energies proportional to the spatial extent, l , the pressure given by

$$P \equiv t \frac{\partial}{\partial l} \ln Z = \frac{\partial}{\partial A} \ln Z = -\frac{1}{N} \langle C_r^{(2)} \rangle, \quad (2)$$

is negative.

The partition function for $SU(2)$ is simple and given by

$$Z = \sum_{\lambda=0}^{\infty} e^{-\frac{(\lambda^2+2\lambda)A}{4}} = \frac{1}{2} e^{\frac{A}{4}} \left[\sum_{\lambda=-\infty}^{\infty} e^{-\frac{\lambda^2 A}{4}} - 1 \right] = \frac{1}{2} e^{\frac{A}{4}} \left[\sqrt{\frac{4\pi}{A}} \sum_{\lambda=-\infty}^{\infty} e^{-\frac{4\pi^2 \lambda^2}{A}} - 1 \right]. \quad (3)$$

The asymptotic behavior of the equation of state is

$$\frac{Pl}{t} = -\frac{3}{4} \frac{l}{t} e^{-\frac{3l}{4t}} \quad \text{as } l \rightarrow \infty, \quad (4)$$

and

$$\frac{Pl}{t} = -\frac{1}{2} \quad \text{as } l \rightarrow 0. \quad (5)$$

The behavior at large l is dominated by a few low lying energy states where as the behavior at small l comes from a sum over all states and could be interpreted as the equipartition limit with the number of degrees of freedom being 1 for $SU(2)$. The cross-over from the behavior on a large circle to a small circle is shown in Figure 1.

Expecting that the equipartition limit is given by

$$\frac{Pl}{t} = -\frac{N-1}{2} \quad \text{as } l \rightarrow 0, \quad (6)$$

for all N , we define

$$Q(\alpha) \equiv -\frac{2Pl}{(N-1)t}; \quad \text{with } \alpha = \frac{Nl}{t}, \quad (7)$$

and study this quantity in this paper.

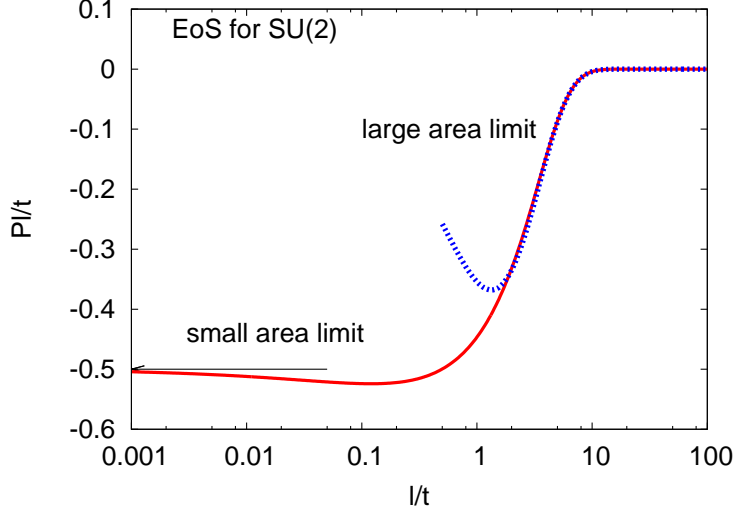


FIG. 1: The equation of state for $SU(2)$ gauge theory on a two-dimensional torus is shown as the solid curve. The asymptotic values of Pl/t at small area is -0.5 . At very large area, Pl/t behaves as $0.75 \exp(-0.75l/t)l/t$, which is shown as the dotted curve. There is a cross-over between the two limits.

II. SUMMARY OF RESULTS

We will show the following results in this paper using a numerical simulation of the partition function in Eq. (1):

1. $Q(\alpha)$ falls on a universal curve as $N \rightarrow \infty$.
2. $Q(\alpha)$ goes to zero as α goes to infinity. This result implies that the pressure at infinite N is zero for all l at any t as long as one takes $N \rightarrow \infty$ keeping l and t finite and is consistent with physics being independent of temperature and spatial extent in the infinite N limit [4, 5].
3. $Q(\alpha)$ goes to unity as α goes to zero. This limit is reached from a finite l and t only at finite N .
4. There is a cross-over point defined as a peak in the susceptibility,

$$\chi = A \frac{\partial}{\partial A} Q = \alpha \frac{\partial}{\partial \alpha} Q. \quad (8)$$

(a) The large l side of the cross-over is dominated by representations where $C_r^{(2)}$ are of $\mathcal{O}(N)$. This is the case of interest for all non-zero l at infinite N and studied in [3].

(b) The small l side of the cross-over is dominated by representations where $C_r^{(2)}$ are of $\mathcal{O}(N^2)$.

5. Since the value of Q at infinite N and $l = 0$ (or equivalently $t = \infty$) depends on the approach to the limit, $N \rightarrow \infty$ and $l \rightarrow 0$, there is a first order transition confirming the argument in [6].

III. PROPERTIES OF CASIMIR FOR SU(N)

The representations of $SU(N)$ are specified by the sequence of integers $\Lambda_r = (\lambda_1, \lambda_2, \dots, \lambda_{N-1})$, subjected to the ordering $\lambda_i \geq \lambda_{i+1}$ and the value of $C_r^{(2)}$ is

$$C_r^{(2)} = \sum_{i=1}^{N-1} \lambda_i^2 - \sum_{i=1}^{N-1} i \lambda_i - \frac{\lambda^2}{N} + (N+1)\lambda \quad \text{where} \quad \lambda = \sum_{i=1}^{N-1} \lambda_i. \quad (9)$$

The maximum and the minimum value of Casimir, given the constraint that λ has to be kept fixed, would be used in the subsequent sections. The representation with the maximum value of $C_r^{(2)}$ for a given λ is given by

$$\Lambda_{\max} = (\lambda, 0, \dots, 0). \quad (10)$$

The minimum value of $C_r^{(2)}$ is given by the sequence Λ_{\min} :

$$\lambda_i = \begin{cases} \lfloor \frac{\lambda}{N-1} \rfloor + 1 & \text{if } i \leq k \equiv \lambda - (N-1) \lfloor \frac{\lambda}{N-1} \rfloor \\ \lfloor \frac{\lambda}{N-1} \rfloor & \text{if } i > k. \end{cases} \quad (11)$$

To prove that the two sequences extremize the Casimir, note that the Casimir decreases under the transformation $(\lambda_1, \lambda_2, \dots, \lambda_i, \dots, \lambda_j, \dots, \lambda_{N-1})$ to $(\lambda_1, \lambda_2, \dots, \lambda_i - 1, \dots, \lambda_j + 1, \dots, \lambda_{N-1})$ for $j > i$, provided this transformation is allowed. Such a transformation is not possible for Λ_{\min} . Similarly, the reverse of that transformation is not possible on Λ_{\max} . One can prove by contradiction that Λ_{\min} and Λ_{\max} are unique to satisfy these properties.

We have shown the behaviour of the maximum and the minimum value of $C_r^{(2)}$ as a function of λ in Figure 2. The minimum of $C_r^{(2)}$ shows a quasi-periodic behaviour, with

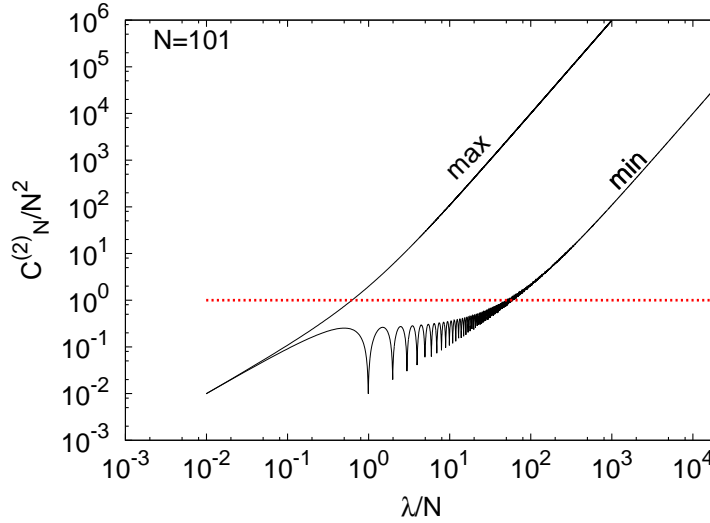


FIG. 2: Behaviour of Casimir as a function of λ . The upper solid curve is the maximum value of Casimir given a value of λ , as a function of λ . Similarly, the lower solid curve is the minimum value of Casimir given a value of λ , as a function of λ . The dotted line is where $C_r^{(2)} = N^2$.

troughs at $\lambda = qN$ for integer q . The values of Casimir at these troughs are

$$C_{\min} = N \left(1 + \left\lfloor \frac{q}{N-1} \right\rfloor \right) \left(2q - \left\lfloor \frac{q}{N-1} \right\rfloor (N-1) \right), \quad (12)$$

whose dependence on N is linear for q between two multiples of $(N-1)$ and is quadratic for q that are multiples of $(N-1)$. On very large circles (or at very low temperatures), one would expect that only the excitations around these troughs at small q would be important. On very small circles (or at very high temperatures), large values of q would become accessible, where all possible Casimir are $\mathcal{O}(N^2)$. This is the region above the red dotted line in Figure 2 where $C_r^{(2)}$ is larger than N^2 . Qualitatively, this is the difference one might expect between the low and high temperature phases.

IV. HEAT-BATH ALGORITHM

We simulated the partition function in Eq. (1) by updating Λ_r by the heat-bath algorithm. Each heat-bath update is a sequence of local updates from λ_1 to λ_{N-1} , in that order, such that the ordering of λ_i is preserved. For the local update of λ_i , the probability distribution

of λ_i is given by a discrete version of the Gaussian distribution

$$T(\lambda_i) \propto e^{-(\lambda_i - \mu_i)^2 / 2\sigma^2}, \quad (13)$$

subject to the condition $\lambda_{i+1} \leq \lambda_i \leq \lambda_{i-1}$ for $i > 1$ and $\lambda_2 \leq \lambda_1$. The μ_i and σ_i for the above discrete Gaussian distribution are functions of the rest of the λ_i 's forming the heat-bath:

$$\mu_i = \frac{\bar{\lambda} + N \left(\frac{2i-N-1}{2} \right)}{N-1} \quad \text{and} \quad \sigma^2 = \frac{N^2}{2A(N-1)}, \quad (14)$$

where $\bar{\lambda} = \sum_{j \neq i} \lambda_j$. For $i > 1$, the set of allowed values for λ_i is bounded from above and below. Hence, we included all the allowed possibilities weighted by Eq. (13) as candidates for the update. Since Eq. (14), along with the inequality $\lambda - \lambda_1 < (N-2)\lambda_2$, implies that $\mu_1 < \lambda_2$, the probability for λ_1 is a monotonically decreasing function. This enables one to put an upper cut-off on λ_1 . In our calculation, we used an upper cut-off of $\lambda_2 + 3\sigma$. We also checked that changing this value to $\lambda_2 + 10\sigma$ does not cause any statistically significant changes. Since a representation r and its conjugate representation \bar{r} have the same Casimir, one can do an over-relaxation step by a global update $\lambda'_i = \lambda_1 - \lambda_{N-i+1}$.

In our simulations, the successive measurements were separated by 100 iterations of 2 heat-bath and 1 over-relaxation steps. The first 2000 measurements were discarded for thermalization. In this way, we collected 10^4 configurations of Λ_r at all area and N .

V. RESULTS

In the top panel of Figure 3, we show the behaviour of Q as a function of the scaled area α for various values of N . The important thing to notice is that Q has a large- N limit when plotted as a function of α . For $\alpha \ll 1$, Q seems to approach 1 for all N . This is in agreement with our intuition based on the equipartition theorem. The non-trivial observation is that this cross-over to the equipartition limit happens at a finite value of α in the large- N limit. For $\alpha \gg 1$, Q seems to behave as $N^{-1} \exp(-\sigma\alpha/N)$ for a constant $\sigma \approx 0.81$ in the large- N limit. This is shown in the bottom panel of Figure 3. Thus, it can also be seen as a cross-over from strong-coupling regime, which has a scale σ , to the weak-coupling regime with no underlying scale.

We determined the cross-over point α_c using the peak-position of the susceptibility χ , after interpolating using multi-histogram reweighting. We show χ as a function of α in

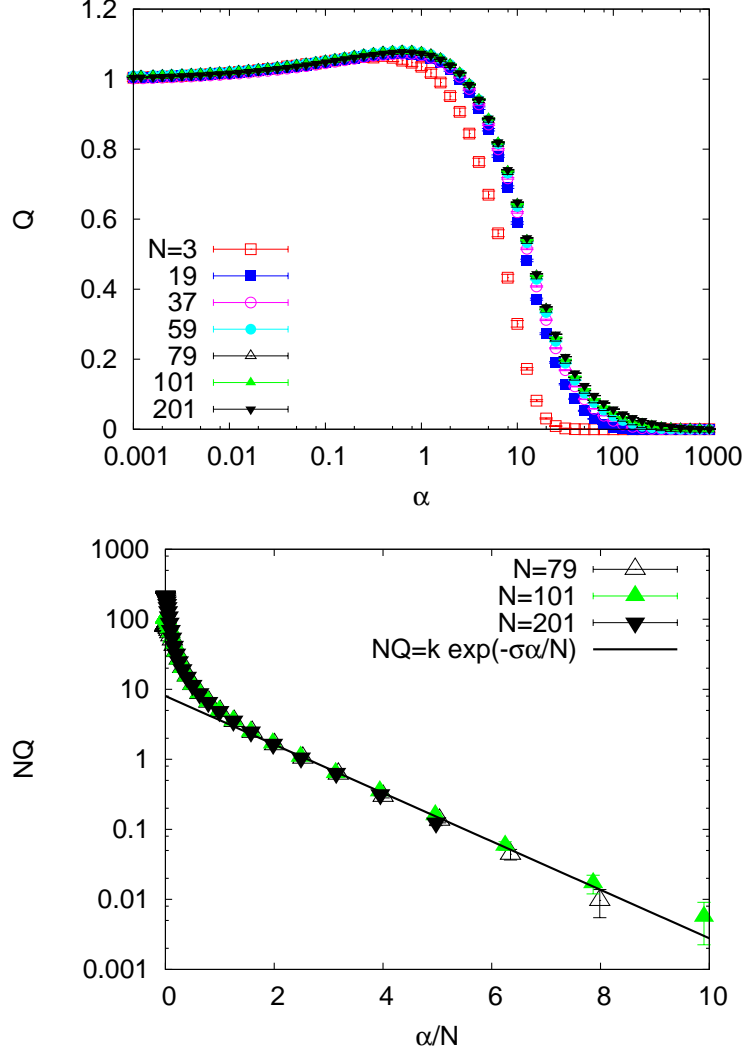


FIG. 3: Q as a function of the scaled area $\alpha = NA$ is shown in the top panel. It is seen that Q as a function of α has a large- N limit. For very small values of α , Q approaches 1. In the bottom panel, the large area behaviour of Q in the large- N limit is shown. In this case, QN behaves as $\exp(-\sigma\alpha/N)$.

Figure 4 for various N . The susceptibility also has a large- N limit when plotted as a function of α . The peak positions of susceptibility for $N > 19$ agree within errors, giving us an estimate $\alpha_c = 12.1(2)$. This implies that the cross-over area $A_c = \alpha_c/N$ shifts to smaller values at larger N . The width of the susceptibility when expressed in terms of the area A decreases inversely as N . This is characteristic of finite volume scaling near a first order phase transition, with the large- N limit replacing the thermodynamic limit in this case.

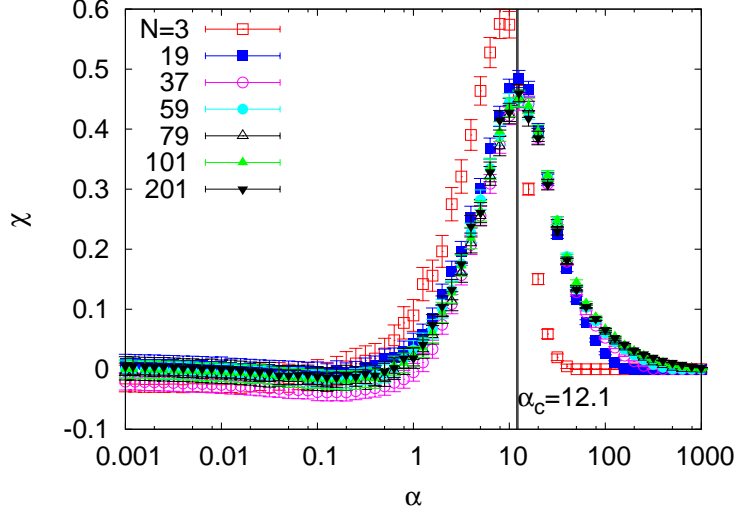


FIG. 4: Susceptibility χ as a function of the scaled area $\alpha = NA$. The cross-over coupling α_c is shown by the vertical line.

The reason for this cross-over can be understood from the scatter plot of $C_r^{(2)}$ versus λ measured during the course of the Monte Carlo run using a value of α . Such scatter plots at various α are shown in Figure 5 for two different N . We also show the maximum and minimum value of Casimir at a fixed λ , as a function of λ . As discussed earlier, the minimum Casimir shows a quasi-periodic behaviour forming wells with a periodicity N . At large values of α , the representations near the troughs of these wells at small values of λ get populated. The representations within these wells are sparse, and this discreteness govern the large area behaviour. At very small area, the most probable $C_r^{(2)}$ moves away from the line of minimum $C_r^{(2)}$ and remains in a region where one can approximate the distribution of Casimir by a continuum. The cross-over between the two behaviours is what shows up as a peak in χ . As discussed in Section III, the Casimir near the troughs at small λ is of $\mathcal{O}(N)$, while the Casimir at very large λ is of $\mathcal{O}(N^2)$. As shown by the dotted line in Figure 5, this cross-over at $\alpha \approx 12.1$ roughly occurs when the dominant behaviour $C_r^{(2)}$ changes from $\mathcal{O}(N)$ to $\mathcal{O}(N^2)$.

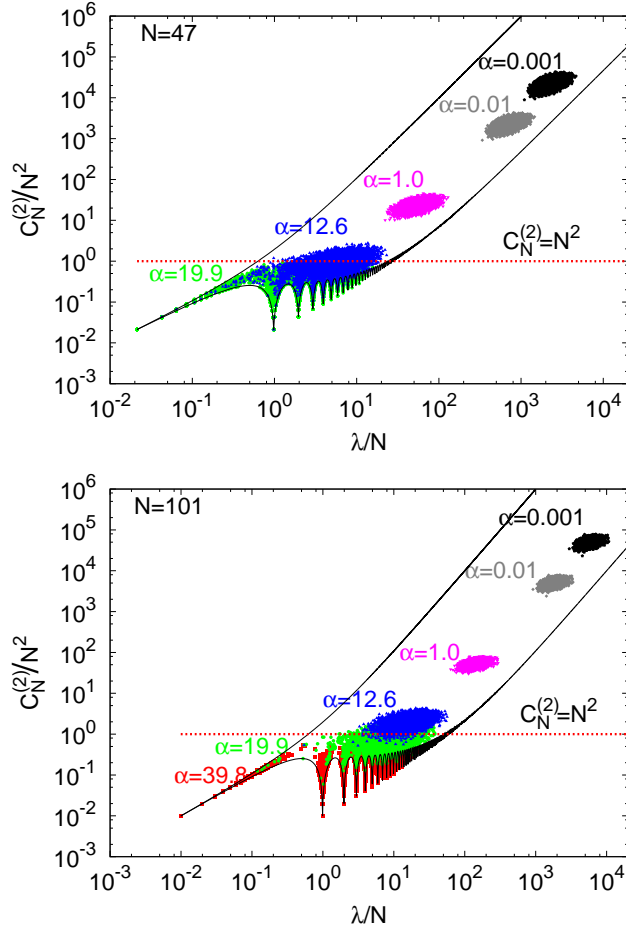


FIG. 5: Scatter plot of $C_r^{(2)}/N^2$ versus λ/N at various area A . The top panel is for $N = 47$ and the bottom one for $N = 101$. Each point corresponds to a $C_r^{(2)}$ and λ measured in the course of Monte Carlo simulation at a particular α specified by the color. The upper and lower solid curves are the maximum and the minimum value of $C_r^{(2)}$ at a given λ respectively.

VI. CONCLUSIONS

Yang-Mills theory in two dimensions is always in the confined phase. We focused on the quantity, $Q = -\frac{2Pl}{(N-1)t}$, to study the equation of state. We showed that the equation of state shows a cross-over from strong coupling (large spatial extent) to weak coupling (small spatial extent) within the confined phase. Viewed as a function of $\alpha = \frac{lN}{t}$, $Q(\alpha)$ approaches a universal curve as $N \rightarrow \infty$ as shown in Figure 6. This behavior is similar to the Durhuus-Olesen transition [7, 8] with the double scaling limit for the equation of state being $N \rightarrow \infty$ and $l \rightarrow 0$ (or $t \rightarrow \infty$) keeping $\alpha = \frac{lN}{t}$ fixed. There is a line of cross-over, $\frac{lN}{t} = \alpha_c$, extending

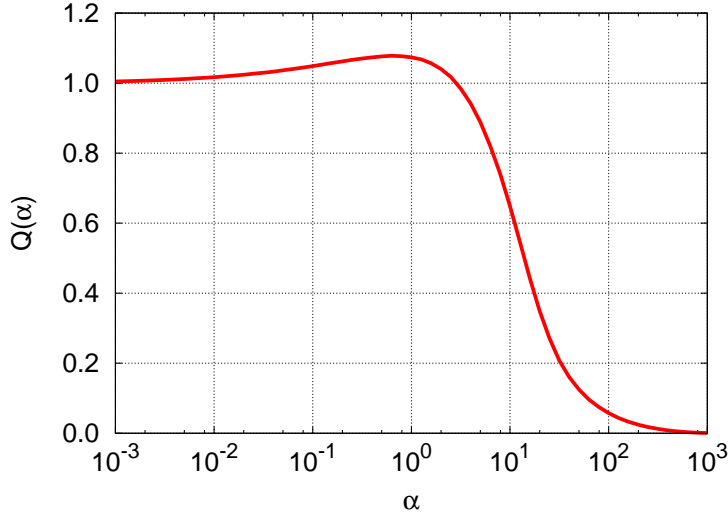


FIG. 6: The large- N limit of Q as a function of α .

from the origin in the $\frac{l}{t} - \frac{1}{N}$ diagram as shown in Figure 7. Well above this line, $Q \ll 1$ and it behaves as $\exp(-\sigma A)/N$. Well below this line, Q is approximately 1. Depending on the slope, α , of the line along which the $N \rightarrow \infty$ and $\frac{l}{t} \rightarrow 0$ limit is taken, the limiting value of Q differs. Specifically, if $N \rightarrow \infty$ limit is taken after the $A \rightarrow 0$ limit is taken, then Q is 1. When the two limits are reversed, Q becomes 0. Therefore, the cross-over along $AN = \alpha_c$ becomes a first order transition at vanishing area in the large- N limit.

The equation of state in four dimensional Yang-Mills theories for several different values of N has been recently studied [9]. The pressure is found to be close to zero in the confined phase. In light of this paper, it would be interesting to perform a careful study of the equation of state in the confined phase in three and four dimensions and see if one can see a cross-over similar to the one seen here in two dimensions.

Acknowledgments

The authors acknowledge partial support by the NSF under grant number PHY-1205396.

-
- [1] A. A. Migdal, Sov.Phys.JETP **42**, 413 (1975).
 - [2] J. Kiskis, R. Narayanan, and D. Sigdel, Phys.Rev. **D89**, 085031 (2014), 1403.1770.

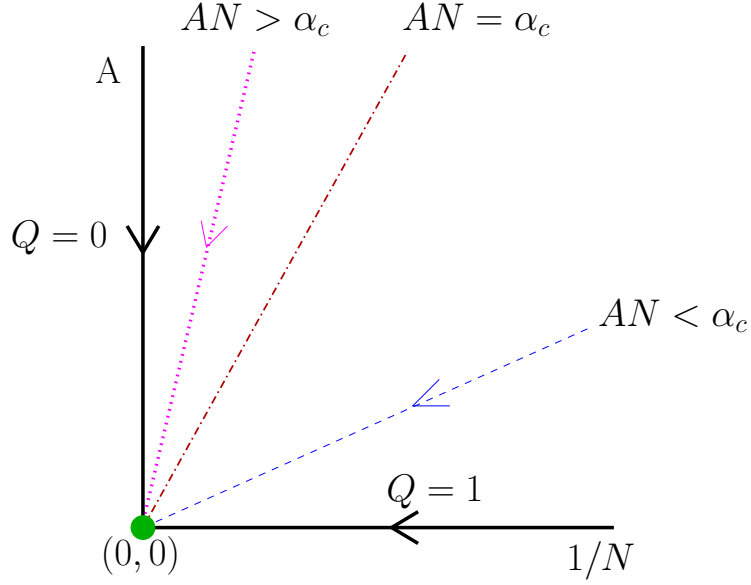


FIG. 7: Phase diagram. Various approaches to vanishing area at large- N are indicated by lines with arrows. The critical value of the slope $AN = \alpha_c$ is shown as the dot-dashed line. For values of $AN \gg \alpha_c$ (the dotted line), Q decays exponentially with area. For values of $AN \ll \alpha_c$ (the dashed line), $Q \approx 1$. In particular, when A is reduced to 0 after taking the large- N limit (*i.e.*, along y -axis), Q vanishes. When the two limits are interchanged (*i.e.*, along x -axis), Q becomes 1.

- [3] D. J. Gross and W. Taylor, Nucl.Phys. **B400**, 181 (1993), hep-th/9301068.
- [4] D. Gross and E. Witten, Phys.Rev. **D21**, 446 (1980).
- [5] T. Eguchi and H. Kawai, Phys.Rev.Lett. **48**, 1063 (1982).
- [6] L. D. McLerran and A. Sen, Phys.Rev. **D32**, 2794 (1985).
- [7] B. Durhuus and P. Olesen, Nucl.Phys. **B184**, 461 (1981).
- [8] R. Narayanan and H. Neuberger, JHEP **0712**, 066 (2007), 0711.4551.
- [9] S. Datta and S. Gupta, Phys.Rev. **D82**, 114505 (2010), 1006.0938.